PHYSICAL REVIEW D **76,** 114510 (2007)

Coulomb gauge Gribov copies and the confining potential

Thomas Heinzl,* Kurt Langfeld,† Martin Lavelle,‡ and David McMullan§

School of Mathematics and Statistics, University of Plymouth, Drake Circus, Plymouth PL4 8AA, United Kingdom

(Received 5 September 2007; published 19 December 2007)

We study the approach, initiated by Marinari *et al.*, to the static interquark potential based on Polyakov lines of finite temporal extent, evaluated in Coulomb gauge. We show that, at small spatial separations, the potential can be understood as being between two separately gauge invariant color charges. At larger separations Gribov copies obstruct the nonperturbative identification of individually gauge invariant color states. We demonstrate, for the first time, how gauge invariance can be maintained quite generally by averaging over Gribov copies. This allows us to extend the analysis of the Polyakov lines and the corresponding, gauge invariant quark-antiquark state to all distance scales. Using large scale lattice simulations, we show that this interpolating state possesses a good overlap with the ground state in the quark-antiquark sector and yields the full static interquark potential at all distances. A visual representation of the Gribov copies on the lattice is also presented.

DOI: 10.1103/PhysRevD.76.114510 PACS numbers: 11.15.Ha, 12.38.Aw

I. INTRODUCTION

The interquark potential is a principal tool in lattice studies of quark confinement [1]. This potential can be understood as composed of antiscreening and screening effects. In perturbation theory the antiscreening structures are paradigm effects of non-Abelian gauge theories and their dominance underlies asymptotic freedom. Screening effects lower the energy but, in perturbative calculations, are seen to be small compared to antiscreening. Nonperturbatively, however, screening due to light quarks starts to dominate at sufficiently large distances implying string breaking. Hence, as was stressed, for example, in [2], confinement with a linearly rising potential at large interquark distances is a feature only of Yang-Mills theory with no light quarks.

Although the potential itself must be gauge invariant, it is initially unclear how to construct it since the heavy fermions are not gauge invariant. On the lattice one measures the vacuum expectation value of the gauge invariant Wilson loop and its large-time behavior [1],

$$W_{rT} \sim \exp\{-TV(r)\}, \tag{1}$$

where r and T denote the spatial and temporal extent of the loop. Wilson's formulation is based on connecting the fermions by a path ordered exponential to produce a single gauge invariant object. However, this is not unique and in this paper we will study other ways of constructing gauge invariant probes of the potential.

To clarify our notation we denote states constructed from the heavy fermionic fields of the theory by $|q_{\boldsymbol{x}}\bar{q}_{\boldsymbol{y}}\rangle$. These are not physical states as they are not gauge invariant. Gauge invariant quark-antiquark states will be denoted by $|Q_{\boldsymbol{x}}\bar{Q}_{\boldsymbol{y}}\rangle$.

As discussed above, the most familiar way to ensure gauge invariance is to link the fermions by a Wilson line. Then the Wilson loop (1) may be found from the transition amplitude

$$W_{rT} \sim \langle \bar{Q}_{\boldsymbol{y}} Q_{\boldsymbol{x}} | e^{-HT} | Q_{\boldsymbol{x}} \bar{Q}_{\boldsymbol{y}} \rangle, \qquad r \equiv |\boldsymbol{x} - \boldsymbol{y}|, \tag{2}$$

which describes the creation of a static quark-antiquark pair at $t = 0$ and its subsequent annihilation at time $t = T$, see Fig. 1.

Inserting a complete set of energy eigenstates, (2) becomes at large times

$$W_{rT} \sim |\langle \bar{Q}_{\boldsymbol{y}} Q_{\boldsymbol{x}} | 0_{\boldsymbol{xy}} \rangle|^2 \exp\{-TV(r)\}, \tag{3}$$

where $|0_{\boldsymbol{xy}}\rangle$ signifies the lowest energy state with a heavy quark and antiquark fixed at $\boldsymbol{x}$ and $\boldsymbol{y}$. For practical computational purposes it is of course important that the matrix element in front is sufficiently large or, put differently, that the state $|Q_{\boldsymbol{x}}\bar{Q}_{\boldsymbol{y}}\rangle$ has a substantial overlap with the true quark-antiquark ground state. Gauge invariance alone does not ensure this and, in particular, Wilson loops do not have

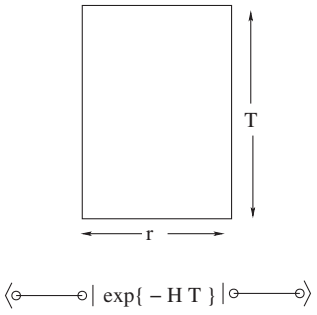

FIG. 1. The static interquark potential from unsmeared Wilson loops.

*theinzl@plymouth.ac.uk
†klangfeld@plymouth.ac.uk
‡mlavelle@plymouth.ac.uk
§dmcmullan@plymouth.ac.uk

such a strong overlap. This is remedied on the lattice by the technique of ''smearing'' [3–5].

Although Wilson loops are gauge invariant and hence potentially physical they *cannot* be interpreted as amplitudes connecting *separately* physical, *single* quark and antiquark states. This is symbolically displayed in Fig. 1 by the lines connecting the external sources (small circles). However, in the perturbative sector physically distinguishable constituent structures are expected [6]. To incorporate this constituent picture into the description of the potential we would require a gauge invariant quark state $|Q_x\rangle$ built out of the heavy, but gauge dependent, fermionic state $|q_x\rangle$.

Such an approach was, in fact, initiated by Dirac [7] many years ago in QED and during the last decade or so this idea has been developed into a fully fledged alternative approach to charges in gauge theories [6,8–10]. The process of constructing a gauge invariant quark from the matter states $|q_x\rangle$ is called ''dressing'' and details of the construction will be summarized in the next section. We will see that the dressing for a static charge takes its simplest form in Coulomb gauge. In that gauge, the fermionic state $|q_x\rangle$ itself captures the dominant gluonic contribution to the perturbative quark constituent of our quark-antiquark configuration. As such, the state $|q_x\bar{q}_y\rangle$ evaluated in Coulomb gauge has a large overlap with the true quark-antiquark ground state, $|0_{xy}\rangle$, at short distances.

This observation allows us to develop an alternative to the unsmeared (or ''thin'') Wilson loop description of the quark-antiquark system. We can now make the gauge invariant identification that for heavy static quarks,

$$|Q_x\bar{Q}_y\rangle|_{\partial_i A_i=0} = |q_x\bar{q}_y\rangle. \tag{4}$$

This is gauge invariant as long as each orbit of the gauge group has one unique representative satisfying the Coulomb gauge condition. Thus the expectation value of the Hamiltonian in the state (4) should give an alternative approach to the interquark potential, see Fig. 2.

An immediate question, which we will address in this paper, is to what extent does the good perturbative overlap found in Coulomb gauge extend to the nonperturbative regime? If it does, then, as well as producing an alternative to smearing, we can start to address issues related to the details and range of validity of the constituent quark picture.

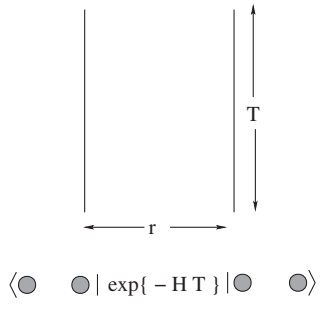

FIG. 2. The static interquark potential from dressed quarks.

In this paper we will test this approach to the interquark potential. That is, we will use Coulomb gauge fermions to measure the potential. On a lattice this means that we first take a Coulomb dressed $Q\bar{Q}$ state on a time slice separated by a distance r and let it evolve during a time interval T, see Fig. 2. This yields a correlator of two separate finite length Polyakov lines with link variables in Coulomb gauge. The correlation of finite length Polyakov lines was first studied on the lattice by Marinari *et al.* in [11]. They considered SU(3) gauge theory and obtained an upper limit for the string tension which overestimated the true value by roughly 50%. It was recently confirmed [for an SU(2) gauge theory] that finite length Polyakov line correlators indeed yield the correct value for the full string tension [12]. One of the goals of this paper is to apply this approach not just to the string tension but to the full interquark potential. Using both perturbation theory and lattice gauge simulations, we will find that the potential between two Coulomb dressed quarks and that obtained from Wilson loops are in good agreement.

An intriguing aspect of the present investigation is the obvious physical fact that the constituent picture has a limited range of validity. Thus any interpretation of the interquark potential as that arising between two physical quarks must break down. It has been argued in Refs.[6,10] that this is consistent with the observation that the gauge invariance of the dressed charges breaks down nonperturbatively due to Gribov copies [13,14]. In this regime the potential defined by the finite length Polyakov lines can only be interpreted as arising from the state which corresponds to one gauge invariant, but overall colorless, object. However, it is not *a priori* obvious that the residual gauge invariance of the states (4) due to copies will let us extract a potential, let alone the confining one. Therefore, another aim of the work reported here is to study how Coulomb gauge Gribov copies affect the interquark potential. One might wonder whether summing over such copies could mean that the potential vanishes (as the construction is not gauge invariant with respect to transformations between Gribov copies). In fact we shall see that we can extract the potential in this way.

The structure of this paper is as follows. First we shall discuss what is known about the perturbative interquark potential. This will include a discussion of the relevant ingredients of the dressing approach to static charges and a summary of their use in identifying the screening and antiscreening structures found in the potential. This will allow us to clarify the significance of Coulomb gauge for the description of static quarks. Then, in Sec. III, the nonperturbative regime will be investigated on the lattice. Results from the use of unsmeared Wilson loops will be compared with those that arise from finite length Polyakov lines in Coulomb gauge. In Sec. IV we will then investigate

in more detail the Gribov copies that arise in this approach and present arguments and evidence for why the interquark potential is insensitive to such copies. We will end with some comments and conclusions.

II. PERTURBATIVE POTENTIAL

A. Dressing approach

In order to be physical, charges must be invariant under gauge transformations which map $\boldsymbol{A} \to {}^{\Omega}\boldsymbol{A}$ and $|q_x\rangle \to \Omega_x|q_x\rangle$. The generic form for a charged single-fermion state is thus given by [15]

$$|Q_x\rangle \equiv h_x[\boldsymbol{A}]|q_x\rangle, \tag{5}$$

where the field dependent dressing, $h_x[\boldsymbol{A}]$, must transform as

$$h_x[{}^{\Omega}\boldsymbol{A}] = h_x[\boldsymbol{A}]\Omega_x^{\dagger}, \tag{6}$$

for $|Q_x\rangle$ to be a gauge singlet. Note that the dressing $h[\boldsymbol{A}]$ can be viewed as a field dependent gauge transformation. The invariance of (5) from (6) is a minimal requirement and there are many ways to construct such invariant states. The simplest manner to write down a gauge invariant state involving a fermion-antifermion pair at different points $\boldsymbol{x}$ and $\boldsymbol{y}$ is to connect them by a straight Wilson line. This is, however, not physically attractive and, as the need for smearing on the lattice shows, is also not the best thing to do in practice.

At a more fundamental level, the problem with such a description may already be seen in QED [16] where the potential between two static fermions, separated by a distance $r = |\boldsymbol{x} - \boldsymbol{y}|$ and connected (dressed) by a *string*, is easily calculated to be proportional to $e^2 r\delta^2(0)$. This is a linearly rising potential (with a divergent coefficient) which would imply confinement in QED. However, upon quantisation the associated state is clearly infinitely excited and thus energetically unphysical. On a discrete lattice the coefficient would be finite, but this would still correspond to a highly excited state which will decay. The reason why the energy is so high is that the electric field is only non-zero on the path of the Wilson line, e.g.,

$$\boldsymbol{E}(\boldsymbol{x}) = \delta^2(\boldsymbol{x}_\perp)\theta(x_3)\boldsymbol{n}, \tag{7}$$

where $\boldsymbol{n}$ is the unit vector in the x_3 direction and $\boldsymbol{x}_\perp = (x_1, x_2)$. The large energy of such thin strings is exactly the reason why smearing Wilson lines is numerically efficient in lattice calculations of the interquark potential: It improves the overlap with the ground state [3–5].

Instead of this we look for a physically motivated description of the dressing of two static charges [17]. We demand that a dressed state is gauge invariant and static as an asymptotic state [8,9]. This produces a dressing which factors into two parts:

$$h = e^{i\kappa}e^{i\chi}. \tag{8}$$

For a static charge, χ is the field dependent transformation into Coulomb gauge. This part of the dressing we also call the "minimal" dressing since the state $e^{i\chi(x)}|q_x\rangle$ is gauge invariant on its own. Hence, its $Q\bar{Q}$ analogue,

$$|Q_x\bar{Q}_y\rangle \equiv e^{i\chi(x)}e^{-i\chi(y)}|q_x\bar{q}_y\rangle, \tag{9}$$

may be expected to have a large overlap with the true $Q\bar{Q}$ ground state $|0_{xy}\rangle$ (involving the full dressing). The additional part of the dressing, κ, is the time integral of the χ rotated A_0 component of the potential. So in Coulomb gauge it is just the (long) Polyakov line of A_0 from the current time to infinity.

It turns out to be a nontrivial task to find a closed expression for χ, the transformation into Coulomb gauge in the non-Abelian case. It is, however, simple to obtain a perturbative expansion for χ to high orders. Absorbing the coupling, g, into the vector potential, the minimal dressing at leading order (LO) is

$$\chi = \frac{\partial_i A_i}{\nabla^2} + \mathcal{O}(g^2). \tag{10}$$

In the Abelian limit this is the result proposed by Dirac [7] to describe a static electron. At next-to-leading order (NLO) and beyond we have

$$\chi = \chi_1 + \chi_2 + \chi_3 + \mathcal{O}(g^4), \tag{11}$$

where explicit expressions for the χ_n's can be found in [6,10]. Given this solution for χ, it is then reasonably straightforward to construct the additional part of the dressing to the same order in the coupling by using χ to gauge rotate A_0. This perturbative construction can be extended to an arbitrary order, however, the above suffices to calculate the NLO potential.

A fermionic field dressed by (8) has two independently gauge invariant structures: κ and the minimally dressed fermion. Given these separately gauge invariant terms, it is instructive to investigate their relative contributions to the potential. The potential between two such dressed quarks is found by sandwiching the Yang-Mills Hamiltonian between states of a dressed quark and antiquark spatially separated by a distance r. As in QED, the LO dressing generates the Coulombic electric field typical of short distances [6] and the additional part of the dressing makes no contribution here. So to LO we find

$$V_{\mathrm{LO}}(r) = \langle\bar{Q}_y Q_x|H_{\mathrm{YM}}|Q_x\bar{Q}_y\rangle - E_0 = \frac{g^2 C_F}{4\pi r}. \tag{12}$$

Here, E_0 collectively denotes contributions independent of the distance r. As usual, C_F denotes the quadratic Casimir in the fundamental representation. The result (12) corresponds to a one-gluon exchange at tree level as will be briefly discussed in the following subsection.

At NLO we focus on the minimally dressed quark where we only retain the Coulomb dressing. The higher order terms in the minimal dressing (11) modify the essentially

Abelian result (12) and generate the paradigm antiscreening effects which underlie asymptotic freedom. In momentum space [18], working in an arbitrary covariant gauge [19] in d spatial dimensions, the chromo-electric commutators produce at NLO the correction

$$-\frac{3g^4 C_F C_A k_i k_j}{\boldsymbol{k}^4}\int\frac{d^dp}{(2\pi)^d}\frac{1}{(\boldsymbol{k}-\boldsymbol{p})^2}iD^{TT}_{ij}(\boldsymbol{p}), \tag{13}$$

where $iD^{TT}_{ij}(\boldsymbol{p})$ is the gauge invariant two-point function of the transverse components $\boldsymbol{A}^T$ of the spatial vector potential and C_A is the quadratic Casimir in the adjoint representation. The potential from the minimal dressing at this order in perturbation theory thus becomes

$$V^{\min}_{\mathrm{NLO}}(\boldsymbol{k}) = \frac{g^2 C_F}{\boldsymbol{k}^2}\left\{1+\frac{g^2 C_A}{48\pi^2}12\ln\left(\frac{\mu^2}{\boldsymbol{k}^2}\right)\right\}, \tag{14}$$

where μ is a renormalization scale. The factor of 12 in front of the logarithm demonstrates that the minimal dressing description yields the dominant *antiscreening* part of the quark potential which is thus generated by the glue needed to make quarks gauge invariant. The expected factor of 11 in the true ground state (familiar from the β function) requires an additional -1 term which is produced by screening due to gauge invariant glue—recall that the additional dressing, κ, is gauge invariant, see [20]. The sign of this smaller effect shows that it lowers the overall energy.

In three dimensions [21] the minimal ressing generalizes this antiscreening/screening divide in the interquark potential despite the fact that this super-renormalizable lower dimensional theory has a vanishing β function. It is noteworthy that the relative weighting of the divide at NLO is almost identical in both three and four dimensions. The renormalization of these physical descriptions of charges has been investigated at next-to-NLO (NNLO) and a cancellation of nonlocal divergences was shown [22]. This was a highly nontrivial check of the construction.

We note also that the arbitrary path dependence of $Q\bar{Q}$ states dressed by a Wilson line may be factorized order by order in perturbation theory. This yields a product dressing consisting of a gauge invariant, but path dependent, gluonic term and a separately gauge invariant structure of two fermions dressed with the above minimal (or Coulomb) dressing [23].

B. Wilson loop approach

To make the transition from the dressing description to the lattice formulation, it is helpful to briefly recapitulate the perturbative route to the potential in terms of Wilson loops, Polyakov lines, and Feynman graphs as initiated in [24] and reviewed in [25]. A path integral definition of the static interquark potential $V(r)$ may be given as follows. We consider the partition function

$$Z[\rho] = \int \mathcal{D}A \exp\left\{-[S_{\mathrm{YM}} + (\rho, A^0)]\right\} \tag{15}$$

in the presence of a static external $q\bar{q}$ source (at $\boldsymbol{x}$ and $\boldsymbol{y}$, respectively),

$$\rho^a_{xy}(z) = -gT^a[\delta(z-\boldsymbol{x}) - \delta(z-\boldsymbol{y})]. \tag{16}$$

The measure in (15) implicitly contains gauge fixing terms as does the action S_{YM}. The partition function Z is the exponential of the Schwinger functional,

$$Z[\rho] \equiv \exp\{-iW[\rho]\}, \tag{17}$$

which yields the static potential in the large-time limit, $T\to\infty$, plus constant self-energy contributions Σ,

$$W[\rho] \to T[V(\boldsymbol{r}) + \Sigma]. \tag{18}$$

If we define the untraced Polyakov line

$$P_T(\boldsymbol{x}) \equiv \mathrm{T}\exp\left\{-ig\int_0^T dtA_0(t,\boldsymbol{x})\right\}, \tag{19}$$

we may rewrite the amplitude (15) as an expectation value, or more properly a two-point function, given by

$$Z[\rho] = \langle \mathrm{tr}P_T(\boldsymbol{x})P^\dagger_T(\boldsymbol{y})\rangle = \int \mathcal{D}A\,\mathrm{tr}P_T(\boldsymbol{x})P^\dagger_T(\boldsymbol{y})e^{-S_{\mathrm{YM}}}. \tag{20}$$

In contrast to the dressing approach to the potential, gauge invariance is not manifest here since the nonlocal operator $\mathrm{tr}P_T(\boldsymbol{x})P^\dagger_T(\boldsymbol{y})$ transforms nontrivially as the Polyakov lines do not trace a closed loop. However, for some gauge choices (e.g., Landau or Coulomb gauge) one expects the spatial part of the gauge potential to decay sufficiently fast in temporal direction that one can close the integration contours to form a rectangular Wilson loop [26]. Choosing spatial and temporal extent r and T, respectively, the resulting Wilson loop (expectation value) is

$$W_{rT} \equiv \left\langle \mathrm{trP}\exp\left\{-ig\oint_{rT} dx_\mu A^\mu\right\}\right\rangle \sim \exp\{-TV(r)\}, \tag{21}$$

with the final expression being approached in the large-time limit, $T\to\infty$. From this familiar gauge invariant construction, perturbative calculations in *covariant* gauges of the potential have been performed to two loops [27,28].

To connect with the minimal-dressing approach, it is useful to recall the calculation of the perturbative interquark potential in Coulomb gauge [29–32]. Taking into account that the Coulomb gluon propagator has a transverse and an instantaneous part, we have, at NLO,

$V =$ 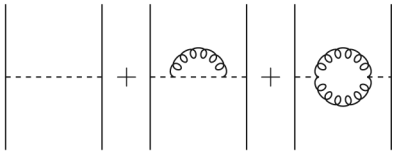 $+\ \mathcal{O}(g^6)\ ,$ (22)

where the dotted lines represent "unphysical" instantaneous Coulomb gluons, A_0, with propagator

$$D_{00}(\boldsymbol{k}) = \frac{i}{\boldsymbol{k}^2}, \tag{23}$$

while the "curly" lines correspond to "physical" transverse gluons A_i^T with propagator

$$D_{ij}^{TT}(k^0, \boldsymbol{k}) = \frac{i}{k_0^2 - \boldsymbol{k} + i\epsilon 2}\left(\delta_{ij} - \frac{k_i k_j}{\boldsymbol{k}^2}\right). \tag{24}$$

The full vertical lines represent the heavy-quark propagators or, equivalently, the untraced Polyakov lines.

Looking at (22) we note that only gluonic two-point insertions contribute. The second diagram corresponds to the minimal contribution to the potential (13) while the third diagram is the smaller screening contribution and may be traced back to the separately gauge invariant dressing, κ, of (8).

Higher n-point functions will only contribute at two-loop order and above in the coupling. We mention in passing that this order has never been worked out in Coulomb gauge as one is faced with a number of difficulties. First, there are severe infrared singularities [33]. Second, integrations over energies (p^0) tend to diverge badly. Third, there are nontrivial contributions from the Faddeev-Popov measure and the Christ-Lee terms [34,35] induced by the curvature of the configuration space. Items two and three seem to be related [36–38].

Working out the diagrams of (22) the potential in momentum space becomes

$$V_{\mathrm{NLO}}(\boldsymbol{k}) = \frac{g^2 C_F}{\boldsymbol{k}^2}\left\{1 + \frac{g^2 C_A}{48\pi^2}(12 - 1)\ln\frac{\mu^2}{\boldsymbol{k}^2}\right\}, \tag{25}$$

where the quantity in brackets determines the running coupling. Asymptotic freedom arises because the *antiscreening* or minimal-dressing contribution yields a factor $+12$, cf. (14), as compared to the -1 from the *screening* vacuum polarization term.

One can understand the different signs at NLO by noting that "physical" particles (like the transverse gluons) in a loop always entail screening by unitarity [39,40]. At small distances this effect is due to virtual particles in the loop. At large distances, however, screening effects may be caused by real particles. This is the case for string breaking in QCD where light dynamical quark pairs pop out of the vacuum and combine with the heavy probe quarks to form heavy-light mesons. This in turn leads to a saturation of the potential at long distances. The same happens in pure gluodynamics if the heavy sources are in higher group representations such that they can be screened by dynamical gluons.

Beyond NLO the separation into screening and antiscreening structures is not so straightforward and the only systematic approach is through the dressing decomposition (8). So, for example, at NNLO physical particles in loops can now contribute to antiscreening [22]. The gauge transformation properties of the dressing ensures that, at all orders in perturbation theory, the separation of forces into screening and antiscreening ones is gauge invariant and hence physical. How this is achieved in the nonperturbative sector is an open question.

III. NON-PERTURBATIVE REGIME

The use of Coulomb gauge in the nonperturbative regime has received much attention recently: There have been investigations using lattice techniques [12,41–46], variational arguments [47–50], Schwinger-Dyson equations [51] and explicit analytic solutions [10]. In particular the so-called Coulomb potential has been studied in great detail. This potential arises from the short Polyakov line correlator (20) in the limit $T \to 0$ [12,44–46] and must not be confused with the full static potential, which we address in the present study. In this section we shall recall the key ingredients of the lattice approach and then see how to extract the interquark potential from finite length Polyakov lines.

A. Numerical setup

The dynamical degrees of freedom are the unitary matrices $U_\mu(x) \in \mathrm{SU}(2)$ which are associated with the links of a N^4 cubic lattice with lattice spacing a. The partition function is given by

$$Z = \int \mathcal{D}U p[U], \quad \text{with} \quad p[U] = \exp\{\beta S[U]\}, \tag{26}$$

where the Wilson coupling β is the only free parameter of the simulation. It multiplies the gauge invariant Wilson action,

$$S[U] = \frac{1}{2}\sum_{\mu<\nu,x} \mathrm{tr} U_\mu(x) U_\nu(x+\mu) U_\mu^\dagger(x+\nu) U_\nu^\dagger(x), \tag{27}$$

which is used throughout this paper. The integration measure is given in terms of single-site Haar measures $dU_\mu(x)$:

$$\mathcal{D}U = \prod_{x,\mu} dU_\mu(x). \tag{28}$$

The latter are invariant under left and right multiplication by SU(2) group elements and normalized to unity, $\int dU_\mu(x) = 1$. This ensures the gauge invariance of $\mathcal{D}U$ and, therefore, of the partition function. Under a gauge transformation $\Omega(x)$, the links change according to

$$U_\mu(x) \to {}^\Omega U_\mu(x) = \Omega(x) U_\mu(x) \Omega^\dagger(x+\mu). \tag{29}$$

In order to impose Coulomb gauge in a lattice simulation, one firstly determines a link dependent gauge transformation, $h(x)$, from the "action principle,"

$$S_{\mathrm{fix}} = \sum_{t,\boldsymbol{x},i} \mathrm{tr}^h U_i(t, \boldsymbol{x}) \xrightarrow{h} \max \tag{30}$$

which, on each gauge orbit, looks for the representative ${}^hU_i$ that is closest to the unit matrix. Note that the sum over times, t, guarantees that this is done term by term on each time slice.

Lattice configurations in Coulomb gauge are then made up from the gauge transformed links ${}^hU_\mu(t, \boldsymbol{x})$. The search for a maximum of the gauge fixing functional $S_{\rm fix}$ is performed with a standard iteration and over-relaxation procedure. For reasonable lattice sizes, present day algorithms will typically find a local (rather than the global) maximum of the gauge fixing action (30) on each orbit.

Starting with the same "seed" configuration $U_\mu(x)$, we might end up in several, almost degenerate, maxima of (30) implying that the lattice definition of the Coulomb gauge configuration is ambiguous. This is the lattice version of the continuum Gribov ambiguity discussed in Sec. I. Two configurations ${}^{h_1}U_\mu(x)$ and ${}^{h_2}U_\mu(x)$ with both $h_1(x)$ and $h_2(x)$ satisfying (30) are hence called Gribov copies of each other. Since we are primarily interested in the effects induced by Gribov copies, we do not employ sophisticated tools such as simulated annealing or Fourier acceleration which are invoked (with little success it must be said) to find the global maximum of (30).

B. Confining potential from unsmeared Wilson loops

The standard way to calculate the potential of a static quark-antiquark pair is to investigate the transition amplitude (2), which we now write as

$$W(r, T) \equiv \langle \bar{Q}_y Q_x | e^{-HT} | Q_x \bar{Q}_y \rangle, \tag{31}$$

where, as before, H denotes the Yang-Mills Hamiltonian, T a Euclidean time interval and $r = |\boldsymbol{x} - \boldsymbol{y}|$ the separation between quark and antiquark. Recall that the latter are connected by a parallel transporter along a straight line. We will evaluate $W(r, T)$ via lattice Monte Carlo simulations employing rectangular Wilson loops (see Fig. 1). As discussed in Sec. I, there are sophisticated lattice techniques [3–5] available for enhancing the overlap, $\langle \bar{Q}_y Q_x | 0_{xy} \rangle$, with the quark-antiquark ground state by using (spatially) smeared Wilson loops. However, since we are not only interested in the static potential *per se*, but also in the overlap of different interpolating states with the true ground state, we refrain from adopting these techniques and content ourselves with a thorough comparison of unsmeared Wilson loops, where there is only an overall gauge invariant quark-antiquark state, with individually dressed Coulombic states as pictorially summarized in Figs. 1 and 2.

Let us first discuss the evaluation of (31). Rewriting the amplitude as

$$W(r, T) \equiv \exp\{-T v(r, T)\}, \tag{32}$$

the interquark potential $V(r)$ emerges as the limit

$$V(r) = \lim_{T \to \infty} v(r, T). \tag{33}$$

The large T limit ensures that excited states which contribute to the matrix element (31) are suppressed. In this limit $v(r, T)$ becomes independent of T. Figure 3 (upper panel) shows $-\ln W(r, T) = T v(r, T)$ as a function of T for several values of r. Deviations from the linear behavior are clearly visible at small values for T. The curves for larger values of r seem to be more affected by excited states.

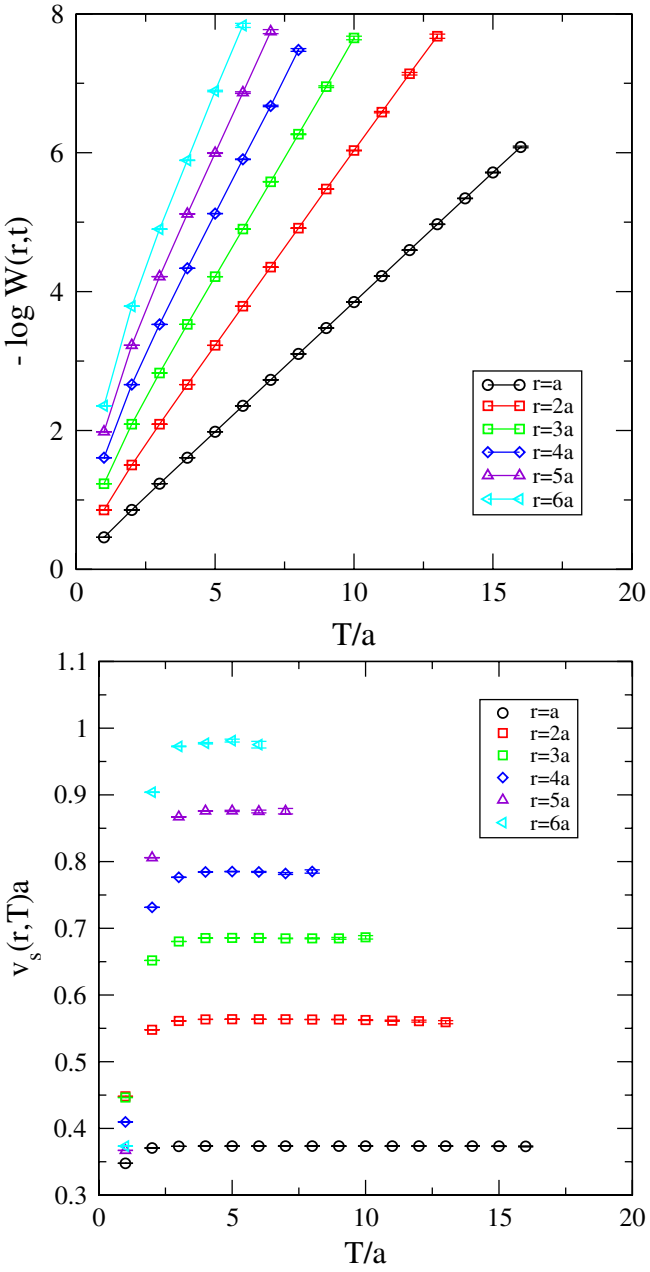

FIG. 3 (color online). The dependence of unsmeared Wilson loops on T; 16^4 lattice, $\beta = 2.4$.

In practice, we fit the logarithm of (32),

$$-\ln W(r,T) \equiv b(r) + V(r)T \tag{34}$$

to a linear function in T (we call this a T fit). Only data points with $T \geq T_{\rm th}$, for some threshold time $T_{\rm th}$, are taken into account. Using small values for the threshold time, say $T_{\rm th} = 2a$, the $\chi^2_T/{\rm dof}$ becomes unacceptably large. This indicates large deviations from linear behavior and implies that the signal is contaminated by contributions from excited states. We have therefore made a more conservative choice for the threshold,

$$T_{\rm th} = 4a, \qquad (16^4 \text{ lattice}, \beta = 2.4) \tag{35}$$

and included only T fits satisfying

$$\chi^2_T/{\rm dof} < 2. \tag{36}$$

The lower panel of Fig. 3 shows

$$v_s(r,T) \equiv [-\ln W(r,T) - b(r)]/T = v(r,T) - b(r)/T \tag{37}$$

as a function of T. It is reassuring to note that, for $T > 4a$, the contributions from excited states are within the statistical error.

The T fit described above also provides us with the desired static interquark potential $V(r)$. Generically, the quark-antiquark pair is aligned along the main crystallographic direction, e.g., {100}, of the lattice. In order to check for artifacts arising due to rotational symmetry breaking, the spatial sides of the Wilson loop were placed along the diagonal axes {110} and {111} as well. Our final result for the unsmeared loop and $T_{\rm th} = 4a$ is shown in the upper panel of Fig. 4. To increase the number of statistically significant data points for $V(r)$ we also relaxed the condition (36) by using the threshold $T_{\rm th} = 3a$, see Fig. 4, lower panel. Also included in this graph is the solid line from the fit to the $T_{\rm th} = 4a$ data. We find that $T_{\rm th} = 3a$ data approach this line reasonably well. Note that the contribution of the excited states in the $T_{\rm th} = 3a$ data yields a slight overestimate of the string tension.

Finally, the potential $V(r)$ is fitted to the universal function

$$V(r) = V_0 - \frac{\alpha}{r} + \sigma r, \tag{38}$$

with offset V_0, Coulombic coefficient α, and string tension σ to be determined (we call this a V fit). Our findings are summarized in Table I.

Not unexpectedly, we find that caution is required when the static potential is extracted from unsmeared Wilson loops: There is a significant contribution from excited states the suppression of which requires a sufficiently large Euclidean time extent T. For the present settings employing a 16^4 lattice and $\beta = 2.4$, we find a 7% drop in the string tension from $\sigma a^2 \approx 0.0908$ to $\sigma a^2 \approx 0.0847$ if we impose the more rigorous bound (36) for the T fit. Note also that calculations which use smeared Wilson loops for an overlap enhancement find smaller values for the string tension, see, e.g., [52]. This indicates that, even for the case

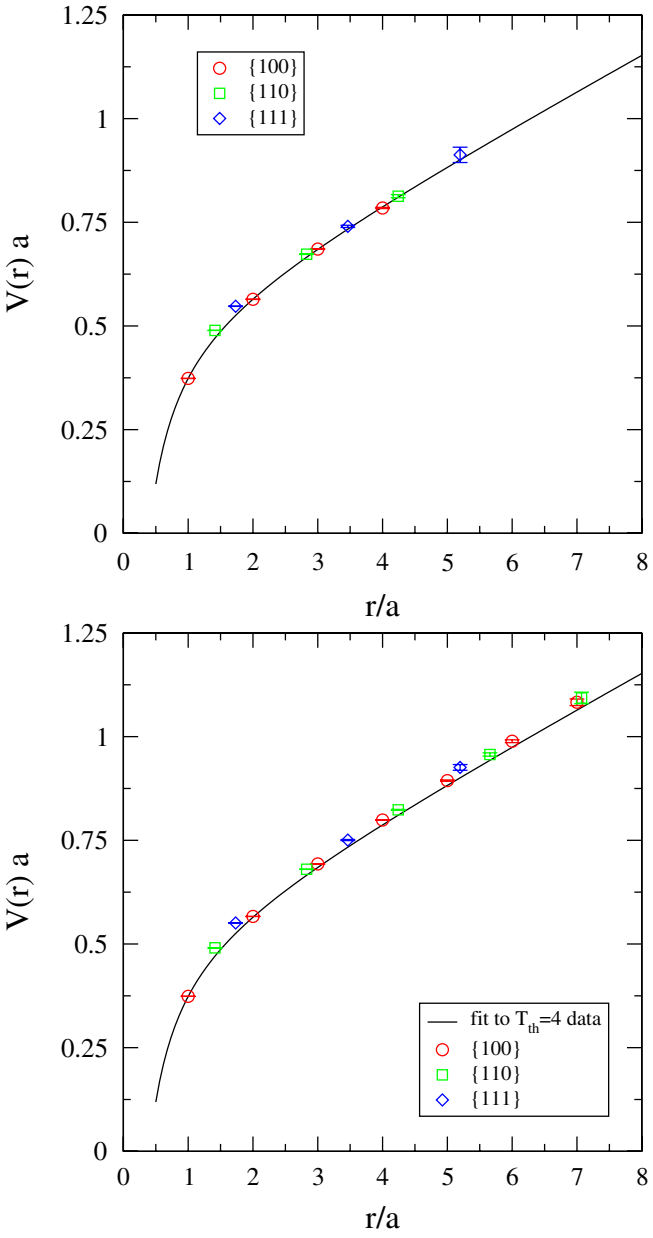

FIG. 4 (color online). The static potential extracted from unsmeared Wilson loops as a function of the quark-antiquark distance r using $T_{\rm th} = 4a$ (upper panel) and $T_{\rm th} = 3a$ (lower panel) as threshold for the T fit; 16^4 lattice, $\beta = 2.4$.

TABLE I. Fit of the static potential to the function (38) for a 16^4 lattice and for $\beta = 2.4$.

	V_0	α	σa^2	$\chi^2_V/{\rm dof}$
$T_{\rm th} = 3a$	0.487(1)	0.204(1)	0.0908(4)	13.0
$T_{\rm th} = 4a$	0.501(3)	0.212(2)	0.0847(8)	4.7

of the more conservative bound (36), there are probably still some contributions from excited states.

C. Confining potential from Coulomb dressed quarks

In what follows we will employ lattice gauge configurations which have been transformed to the Coulomb gauge along the lines described in Sec. III A. Our working hypothesis here is that we can extract the physical interquark potential despite the presence of Gribov copies. The authors of [11,12] found that the large distance part of the potential, i.e., the string tension, is not affected by Gribov copies. However, no physical explanation of this observation was given. Although the copies obstruct the *interpretation* of the resulting potential as that arising between separately invariant single quark sources [6] we shall demonstrate that they do not affect the overlap with the ground state.

The overlap of a Coulomb dressed, single heavy-quark state at $t = 0$ with the analogous state at $t = T$ is given by a finite length Polyakov line (evaluated in Coulomb gauge),

$$ {}^hP_T(\boldsymbol{x}) \equiv \prod_{t=0}^{T} {}^{h[U]}U_0(\boldsymbol{x}, t), \tag{39} $$

where ${}^hU_\mu(x)$ denotes the link after gauge fixing. According to (20) the potential of two static Coulomb dressed quarks can then be extracted from the correlator of two Polyakov lines of finite temporal extent,

$$ C(r, T) \equiv \langle \mathrm{tr}\, {}^hP_T(\boldsymbol{x}) {}^hP_T^\dagger(\boldsymbol{y}) \rangle. \tag{40} $$

This correlator was studied in [12] with an emphasis on the Coulomb (minimal antiscreening) potential obtained from the limit $T \to 0$. In this paper, we will concentrate on the full static potential (large T behavior) and the impact of Gribov copies. For sufficiently large values of T the excited states are suppressed and we expect $C(r, T)$ to be dominated by the true $Q\bar{Q}$ ground state $|0_{xy}\rangle$. Hence, defining quantities analogous to (32) and (33),

$$ C(r, T) \equiv \exp\{-Tu(r, T)\}, \qquad U(r) = \lim_{T\to\infty} u(r, T), \tag{41} $$

we expect $U(r)$ to coincide with the static potential $V(r)$ extracted from unsmeared Wilson loops. The purpose of the present subsection is to scrutinize this expectation by a detailed numerical investigation.

As we will have to deal with gauge fixing ambiguities let us first address the issue of residual gauge invariance. As is appropriate for a Hamiltonian formulation, the Coulomb gauge prescription (30) is implemented on time slices, $t =$ const. Hence, we may still perform spatially homogeneous, purely time dependent residual gauge transformations, $\Omega(t)$, on the gauge fixed links,

$$ {}^hU_\mu(t, \boldsymbol{x}) \to {}^{\Omega(t)h}U_\mu(t, \boldsymbol{x}) = \Omega(t) {}^hU_\mu(t, \boldsymbol{x}) \Omega^\dagger(t), \tag{42} $$

which, in continuum language, obviously leave the (vanishing) divergence of $\boldsymbol{A}(t, \boldsymbol{x})$ invariant.

Let us now convince ourselves that the correlator $C(r, T)$ of (40) is invariant under (42),

$$ \begin{aligned} \mathrm{tr}^{\Omega(t)} P_T(\boldsymbol{x})^{\Omega(t)} P_T^\dagger(\boldsymbol{y}) &= \mathrm{tr}\Omega(0) P_T(\boldsymbol{x}) \Omega^\dagger(T) \Omega(T) P_T^\dagger(\boldsymbol{y}) \Omega^\dagger(0) \\ &= \mathrm{tr} P_T(\boldsymbol{x}) P_T^\dagger(\boldsymbol{y}), \end{aligned} \tag{43} $$

where the links can, in fact, be taken in any gauge. Thus,

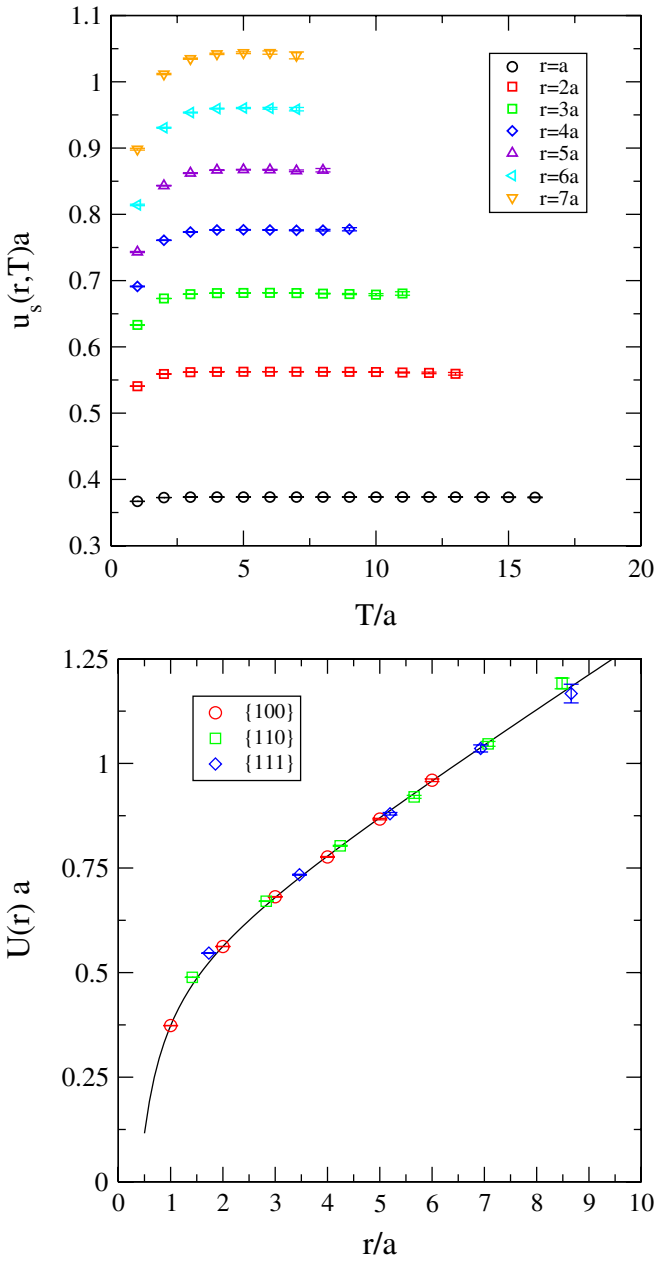

FIG. 5 (color online). $u(r, T)$ extracted from the correlation of finite length Polyakov lines calculated from Coulomb gauge fixed lattice configurations (upper panel). The static potential calculated from finite length Polyakov lines (lower panel). Both on a 16^4 lattice with $\beta = 2.4$.

TABLE II. Fit of the static potential $U(r)$ to the function (38) for a 16^4 lattice and for $\beta = 2.4$.

	V_0	α	σa^2	χ^2_V/dof
$T_{\mathrm{th}} = 3a$	0.505(1)	0.214(1)	0.0827(2)	11.0
$T_{\mathrm{th}} = 4a$	0.510(2)	0.217(1)	0.0807(4)	6.5

$C(r, T)$, and with it the potential $U(r)$ from (41), are not affected by the trivial residual gauge freedom (42).

For a quark trial state which is not completely invariant because of Gribov copies, one might naively expect that the average over gauge copies causes the correlator $C(r, T)$ to vanish. This would imply that the distribution of copies is completely random. Our numerical simulations, however, show that this is not the case: We obtain a clear signal for $C(r, T)$, which is orders of magnitude larger than the underlying noise. We therefore apply the linear T fit to the function $-\ln C(r, T)$ subject to the rigorous bounds

$$T_{\mathrm{th}} = 4a, \qquad \chi^2_T/\mathrm{dof} < 2. \tag{44}$$

The fit results allow us to extract $u(r, T)$ to high accuracy as shown in Fig. 5, upper panel. The outcome is clearly encouraging: Not only is the Gribov noise absent, it also appears that the overlap with the ground state is largely enhanced. In Fig. 5 even the $r = 7a$ data are statistically significant. This is also true for the plot of the static potential $U(r)$ defined in (41). Finally, we have again fitted the parametrization (38) of the potential to the present data (Fig. 5, lower panel). The results of this V fit are listed in Table II.

For comparison, the parameters for the fit with threshold $T_{\mathrm{th}} = 3a$ have also been included. The results seem to be more stable than those from the fits to unsmeared Wilson loop data (cf. Table I). This once again signals the larger ground state overlap of the Coulomb dressed $Q\bar{Q}$ states as compared to the $q\bar{q}$ states linked by an unsmeared Wilson line.

Concluding this subsection we reemphasize the striking fact that Gribov copies seem to have no noticeable effect on the interquark potential. As a result, possible contamination by excited states notwithstanding, it is fair to say that the potentials calculated from unsmeared Wilson loops and from Coulomb dressed quark states do agree.

IV. ON THE IMPACT OF GRIBOV COPIES

In the last section we have shown that the static potentials obtained from finite length, Coulomb dressed Polyakov lines and from unsmeared Wilson loops agree. Our calculations have required a substantial processing of raw numerical data such as the subtraction of divergent self-energies. The question therefore arises whether the agreement between standard and Coulomb gauge calculations also holds for the *bare* finite time amplitudes, $W(r, T)$ and $C(r, T)$ from (32) and (41), respectively.

If this were true, we would be in a much better position to understand the impact of Gribov copies as this issue could be properly addressed before renormalization.

A. Gribov noise

Let us start with a description of the actual numerical procedure which is used to calculate the expectation value of an observable $O[U]$ in Coulomb gauge. Using standard Monte Carlo techniques, a link configuration $\{U\}$ is generated according to the gauge invariant probability distribution $p[U]$, cf. (26). Without gauge fixing an expectation value is calculated as

$$\langle O \rangle = \int \mathcal{D}U p[U] O[U]. \tag{45}$$

If we evaluate this after an arbitrary gauge transformation, $U \to {}^{\Omega}U$, using invariance of the probability measure $\mathcal{D}U p[U]$,

$$\langle O \rangle = \int \mathcal{D}U p[U] O[{}^{\Omega}U] = \int \mathcal{D}U p[U] \int \mathcal{D}\Omega O[{}^{\Omega}U], \tag{46}$$

we obviously obtain zero whenever the projection $\int \mathcal{D}\Omega O[{}^{\Omega}U]$, i.e., the group average of O, vanishes. For gauge *variant* field combinations this is what typically happens.

However, the situation will be different after gauge fixing where, as a result of the gauge fixing algorithm, any seed configuration will change into a Coulomb gauge configuration

$$\{U\} \to \{{}^{h}U\}, \qquad h = h[U], \tag{47}$$

with (yet unknown) probability $P[{}^{h}U]$ characterizing the algorithm. We emphasize that the proper way to interpret the transformation (47) is as a *change of variables* [34] implying curvilinear coordinates and a metric formulation which, however, will not be needed here.

It will be sufficient to *define* the expectation value of an operator $O[U]$ in Coulomb gauge according to

$$\langle\langle O \rangle\rangle \equiv \int \mathcal{D}^h U P[{}^{h}U] O[{}^{h}U], \tag{48}$$

where the double bracket emphasizes that $O[U]$ need not be gauge invariant. Note, however, that the dressed operator $O[{}^{h}U]$ is, by construction, invariant up to Gribov copies as h always picks an orbit representative. If there were no Gribov noise the chosen representative would be unique. This uniqueness is corrupted by the unavoidable randomness inherent in the gauge fixing algorithm implying a *distribution* of representative copies. It is this distribution which we want to study in the following.

To this end let us rewrite the expectation value (48) in terms of the Yang-Mills functional integral. The probability of picking a particular copy ${}^{h}U$ is given by the gauge group average

$$\pi({}^hU|U) \equiv \int \mathcal{D}\Omega \rho({}^hU|{}^\Omega U), \tag{49}$$

which is gauge invariant by *fiat*,

$$\pi({}^hU|{}^\Omega U) = \pi({}^hU|U). \tag{50}$$

The gauge dependent quantity $\rho({}^hU|{}^\Omega U)$ in (49) denotes the (gauge dependent) probability distribution for obtaining the output copy ${}^hU$ when the numerical procedure was initiated with input ${}^\Omega U$ and hence characterizes the gauge fixing algorithm. With these prerequisites, we find for the distribution P in (48):

$$P[{}^hU] = \int \mathcal{D}U \pi({}^hU|U) p[U]. \tag{51}$$

Inserting this into (48) the expectation value becomes

$$\langle\langle O \rangle\rangle = \int \mathcal{D}U p[U] \int \mathcal{D}^hU \pi({}^hU|U) O[{}^hU]. \tag{52}$$

Before we proceed further let us check that we recover the familiar formula under the assumption that there is no Gribov ambiguity. In this case, the gauge fixing algorithm would map U to the unique Coulomb gauge representative ${}^{h_0}U$ implying a sharp distribution

$$\pi({}^hU|U) = \delta({}^hU|{}^{h_0}U), \quad \text{where } h_0 = h_0[U]. \tag{53}$$

In this case, (52) results in the expression,

$$\langle\langle O \rangle\rangle = \int \mathcal{D}U p[U] O[{}^{h_0}U], \tag{54}$$

which is gauge independent by the (assumed) uniqueness of $h_0[U]$.

In the generic case, when Gribov copies are present, (53) is no longer true. Nevertheless, gauge invariance is maintained due to the invariance property (50) of $\pi({}^hU|U)$. This allows for the definition of a gauge invariant average over Gribov copies,

$$\bar{O}[U] \equiv \int \mathcal{D}^hU \pi({}^hU|U) O[{}^hU], \tag{55}$$

which indeed satisfies $\bar{O}[{}^\Omega U] = \bar{O}[U]$. Finally, upon plugging this into (52), the expectation value may be compactly written as

$$\langle\langle O \rangle\rangle = \langle \bar{O} \rangle, \tag{56}$$

where the brackets on the right-hand side indicate the standard average with the Yang-Mills probability distribution, $p[U]$.

Let us apply this now to the finite length Polyakov loop correlator, i.e.,

$$O[U] \equiv C[U] = \mathrm{tr}(P_T(\boldsymbol{x}) P_T^\dagger(\boldsymbol{y})), \tag{57}$$

and analyze its gauge invariant average $\bar{C}[U]$ associated with Coulomb gauge. Since $C[U]$ is gauge dependent it could nevertheless happen that this average ("Gribov mean"),

$$\bar{C}[U] \equiv \int \mathcal{D}^hU \pi({}^hU|U) C[{}^hU], \tag{58}$$

though gauge invariant, actually vanishes when the copies are averaged over. We will show shortly that this is not the case. Therefore, $\bar{C}[U]$ can indeed be interpreted as a nontrivial gauge invariant observable.

Let us consider a specific example. For a 16^4 lattice and $\beta = 2.4$ we have generated a single sample configuration to which we apply a random gauge transformation. The result, call it U is submitted to the gauge fixing algorithm which produces a Gribov copy configuration, ${}^{h_1}U$. With this configuration, we calculate the correlator

$$C_1 \equiv \frac{1}{N^3} \sum_{\boldsymbol{x}} \mathrm{tr}^{h_1} P_T(\boldsymbol{x})^{h_1} P_T^\dagger(\boldsymbol{y}), \tag{59}$$

where $\boldsymbol{y} = \boldsymbol{x} + r\boldsymbol{e}_3$. We choose the distances $r = 3a$ and $T = 4a$ for the present example. Repeating this procedure 200 times, leaves us with observables C_i, $i = 1 \ldots 200$. Their numerical values are distributed as shown in Fig. 6.

Note that for a gauge invariant (i.e., noise free) field combination, such as the plaquette, one would find a δ function distribution according to (53). However, for $C[U]$ in (58) we find a broad distribution with mean μ and standard deviation s given by:

$$\mu = 0.0498(1), \quad \text{and} \quad s = 0.0011(1). \tag{60}$$

A bootstrap analysis was used for the error estimate in

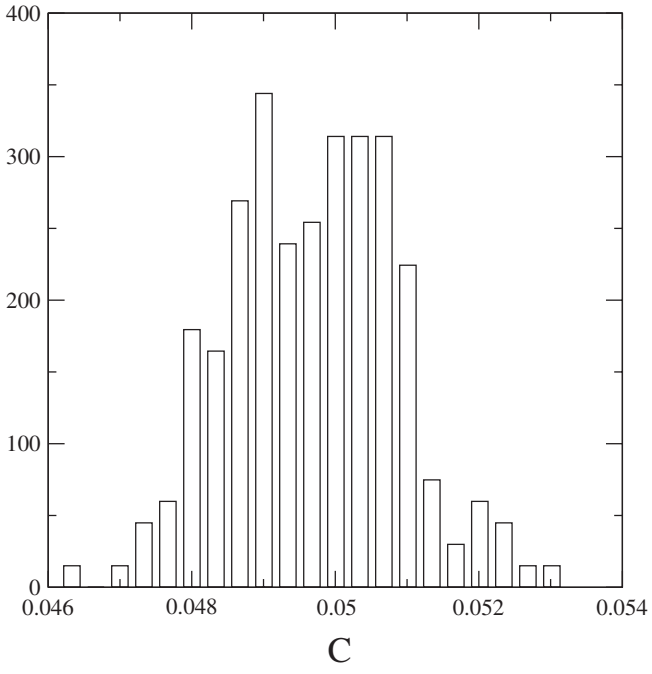

FIG. 6. Gribov noise distribution of the correlator C from (57) for one sample configuration U and distances $r = 3a$ and $r = 4a$.

these values. As they depend significantly on the gauge fixing algorithm as well as the observable under consideration their interpretation in terms of physical quantities is somewhat limited. They do, however, provide information on the impact of Gribov copies since (i) μ significantly differs from zero and (ii) the relative width s/μ of the distribution is only of the order of 2%. This rules out the possibility that the average over Gribov copies induces a null result.

B. Gauge invariant signals from Gribov-noisy data

As a first step, we will investigate the relation between the data from finite length Polyakov lines and gauge invariant Wilson loops. Again using the 16^4 lattice and $\beta = 2.4$, we have generated 10 seed configurations U. For each seed configuration, we produced 10 Gribov copies of it. We have then calculated $r = 3a$ and $T = 4a$ Wilson loops which are averaged over the spatial coordinates. The result is called $W[U]$. For each Gribov copy, the spatial average of finite length Polyakov lines was also obtained (denoted as $C[{}^hU]$). As in the previous subsection, there will be a distribution of values of $C[{}^hU]$ because of the Gribov noise.

This data is shown in Fig. 7. For each seed configuration (and therefore for each value $W[U]$) there is a band of values for $C[{}^hU]$ produced by the Gribov copies. If we assume a perfect correlation of the expectation values, i.e.,

$$\langle\langle C\rangle\rangle \propto \langle W\rangle, \tag{61}$$

the data would be symmetrically scattered around the solid line also shown in Fig. 7. If, on the other hand, the Gribov noise were uncorrelated to the underlying seed configuration, the scatter plot would be homogeneous. Our findings, shown in Fig. 7 upper panel, suggest that a significant correlation survives the Gribov average.

To further test this correlation between finite length Polyakov lines and gauge invariant Wilson loops, we compare $v(r, T)$ from (32) as obtained from unsmeared Wilson loops, with $u(r, T)$ from (41). Figure 7, lower panel, shows the corresponding scatter plot. We clearly observe a linear correlation between the two quantities:

$$u(r, T) = v(r, T) + \epsilon(T). \tag{62}$$

The important observation is that $\epsilon(T)$ does not contribute to the r dependent part of the static potential. Hence, we find that only the unobservable offset of the potential is changed if finite length Polyakov lines are employed rather than unsmeared Wilson lines. This observation has far reaching consequences: Gribov copies will affect the quark self-energies, but their impact on the r dependence of the static potential is limited.

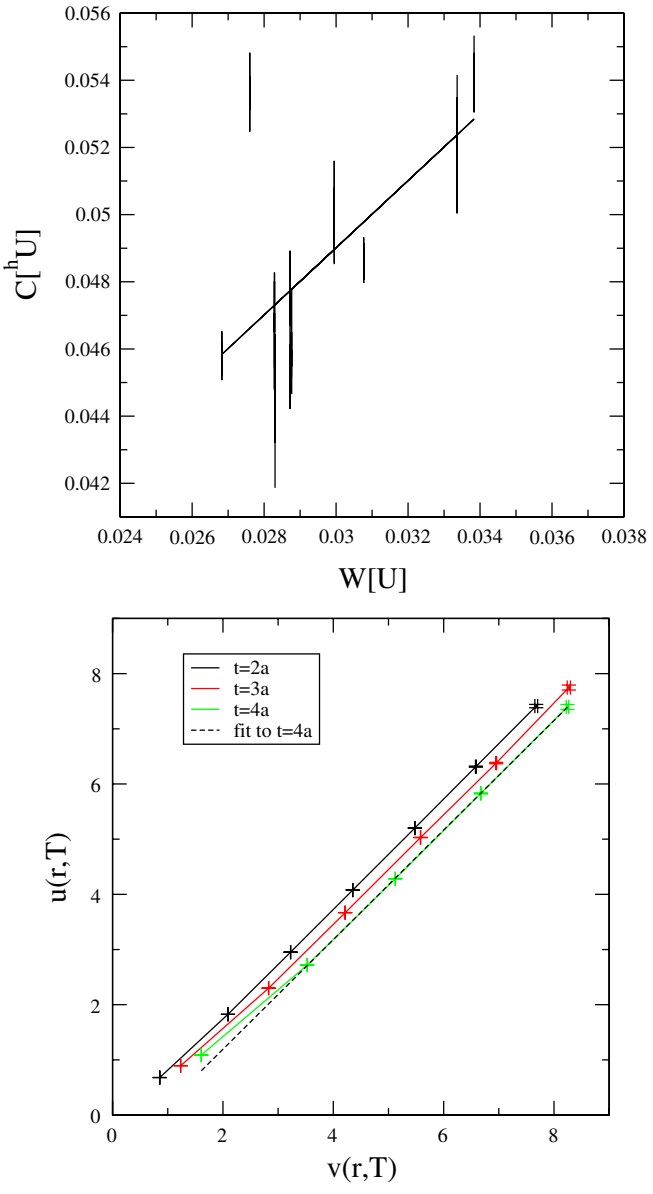

FIG. 7 (color online). Scatter plot for ten seed configurations U (upper panel). Scatter plot of $u(r, T)$, see (41), versus $v(r, T)$, see (32), for several values of r and T (lower panel).

C. Gribov gallery

In order to trace out the origin of the ideal correlations discovered in the previous subsection, let us visualize the spatial dependence of the Gribov copies. This dependence can change the r dependence of the finite length Polyakov line correlator as follows. We note that a similar investigation for the case of Landau gauge was performed in [53]. Generally two different runs of the gauge fixing algorithm result in two different maxima along the orbit of a seed configuration, U_μ. This in turn yields two Gribov copies, say ${}^hU_\mu$ and ${}^{ch}U_\mu$, which are related by a residual copy gauge transformation, c. Knowing that the Coulomb gauge (30) has a trivial residual gauge freedom consisting of purely time dependent gauge transformations (42), we need to distinguish between genuine copies ch and those of the form $\Omega(t)h(x)$ which would also satisfy the

Coulomb gauge condition. We therefore define

$$\tilde{c}(x) = \Omega(t)c(x), \tag{63}$$

and use the purely time dependent degree of freedom $\Omega(t)$ to bring $\tilde{c}$ as close to unity as possible,

$$\sum_{\boldsymbol{x},t} \mathrm{tr}\tilde{c}(\boldsymbol{x}, t) \overset{\Omega(t)}{\rightarrow} \max. \tag{64}$$

This should suppress the contamination by trivial copies. In other words, a space dependent $\tilde{c}(x)$ with $\mathrm{tr}\tilde{c}(x)/2$ not being 1 everywhere signals the presence of a nontrivial Gribov copy. With these prerequisites we can now investigate how such a copy affects the finite length Polyakov loop correlator.

Defining the spatial pure gauge link,

$$M(\boldsymbol{yx}, t) \equiv \tilde{c}^{\dagger}(\boldsymbol{y}, t)\tilde{c}(\boldsymbol{x}, t), \tag{65}$$

the Polyakov line correlator associated with the copy ${}^{ch}U_{\mu}$ may be written as

$$\begin{aligned} C_{\boldsymbol{xy}}[{}^{ch}U] &= \langle \mathrm{tr}\,{}^{ch}P_T(\boldsymbol{x})\,{}^{ch}P_T^{\dagger}(\boldsymbol{y})\rangle \\ &= \langle \mathrm{tr}M(\boldsymbol{yx}, 0)\,{}^{h}P_T(\boldsymbol{x})M^{\dagger}(\boldsymbol{yx}, T)\,{}^{h}P_T^{\dagger}(\boldsymbol{y})\rangle, \end{aligned} \tag{66}$$

This means that, whenever the matrices $\tilde{c}(x)$ differ significantly from unity, an additional nonlocal correlation is induced to the correlator of finite length Polyakov lines.

Figure 8 illustrates the space dependence of $\tilde{c}(x)$ for two generic lattice configurations for $\beta = 2.4$ at a fixed time slice. The density of points in the graph is a direct measure for the deviation of $\mathrm{tr}\tilde{c}/2$ from 1. Although the underlying seed configuration is UV noisy, $\mathrm{tr}\tilde{c}$ changes rather smoothly throughout space. This explains why $M(\boldsymbol{yx})$ is not too different from unity for moderate distances $|\boldsymbol{y} - \boldsymbol{x}|$. Note that $M(\boldsymbol{yx})$ strongly depends on the efficiency of the gauge fixing algorithm in singling out a unique maximum on the gauge orbit. Without adapting the algorithm, there will be also a substantial dependence of $M(\boldsymbol{yx})$ on the volume since the algorithms generically become inefficient for large volumes. This fact can be seen from Fig. 8 where two different volumes have been used in conjunction with the same gauge fixing algorithm. For the larger volume (lower panel), the modulation induced by $M(\boldsymbol{yx})$ is much more pronounced. The finite size effect which we observe here clearly deserves further study. Of particular interest is the question whether the volume dependence is just an algorithmic artifact or whether there is some real physics behind it.

An attractive feature of the Coulomb gauge is the fact that the Gribov link, $M(\boldsymbol{yx}, t)$, is purely spatial (i.e., located in a single time slice t) and thus does not interfere with time evolution and the transfer matrix formalism. Hence, as long as the field combination $C[{}^{h}U]$ does not vanish upon averaging over Gribov copies, this average only affects the definition of the interpolating trial state, $|Q_{\boldsymbol{x}}\bar{Q}_{\boldsymbol{y}}\rangle$. In other words, different gauge fixing algorithms will correspond to different *Ansätze* for the quark-antiquark trial states which might differ in their overlap with the true ground state, $|0_{\boldsymbol{xy}}\rangle$. This is somewhat reminiscent of the situation arising in the process of smearing Wilson lines.

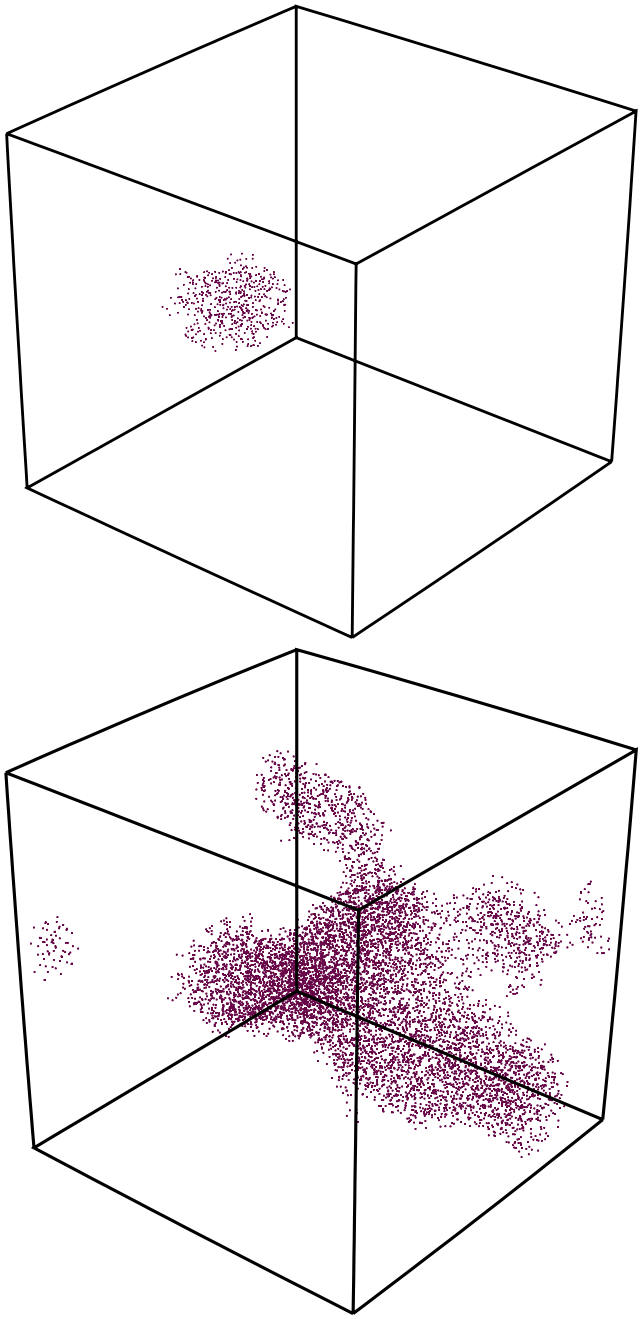

FIG. 8 (color online). Region of space where $\mathrm{tr}\tilde{c}(x)/2$ resulting from (64) significantly deviates from 1, both on a 16^4 lattice (upper panel) and on a 24^4 lattice (lower panel)

V. CONCLUSIONS AND DISCUSSION

In this paper we have developed a formalism based on Coulomb gauge fixing which allows us to incorporate the

ubiquitous Gribov copies in a systematic and gauge invariant way. This has been achieved by defining, for the first time, a Gribov average of gauge variant field combinations.

We have applied this to a thorough lattice investigation of Polyakov lines of finite temporal extent introduced by Marinari *et al.* in [11] and further studied in [12,44–46]. These lines, even if traced, are not often studied on the lattice since their expectation value, without gauge fixing, is zero due to their lack of gauge invariance. Using our formalism, we have shown that, and explained why, they have a physical interpretation when working in Coulomb gauge. This has enabled us to extract the confining interquark potential and to analyze the Gribov copies associated with that gauge and their impact on the overlap with the ground state in the quark-antiquark sector.

We have seen that the value of the string tension obtained from the correlator of finite length, dressed Polyakov lines lies below that obtained from our simulations with unsmeared Wilson loops (compare Tables I and II). This indicates that the Coulomb dressed Polyakov lines are, as we expected, less contaminated by overlaps with higher energy states. Indeed, even using shorter lines in this approach give a smaller string tension than for unsmeared Wilson loops of larger temporal extent.

Many topics brought to light here deserve further exploration. In particular, Gribov copies have been demonstrated not to hinder the measurement of the full quark-antiquark potential in this construction. They merely contribute to the definition of the interpolating quark-antiquark state, and we have demonstrated in this paper that its overlap is even better than that of the state where quark and antiquark are joined by a thin flux line. It would be interesting to study in a more systematic way the contributions of excited states to the finite length Polyakov lines. There is also an obvious extension of this, namely, to use other gauges and so test whether, as we predict, other dressings have a poorer overlap with the true ground state of Yang-Mills theory.

The Gribov induced nonlocality seen in Sec. IV C hinders a proper definition of the constituent quark picture. We would argue that our results support the expected breakdown of a constituent picture of quarks and antiquarks in the confining region. The structure of the copies displayed in Fig. 8, their volume dependence and sensitivity to algorithms therefore merit further investigation. It would also be very interesting to probe the Gribov nonlocality in the high temperature deconfinement regime where the constituent quark picture is expected by many to make sense. In this context, it would also be important to study the relation between the Gribov nonlocality and the confining vortices advocated in, e.g., [54]. If the confining vortices are removed, see [54], do the Gribov copies seen in Fig. 8 vanish with them thereby giving rise to a constituent quark picture?

ACKNOWLEDGMENTS

During the course of this work we benefited from discussions with Anton Ilderton and Andreas Wipf. We thank Philippe de Forcrand for correspondence. We are also indebted to Wolfgang Lutz for a careful reading of the manuscript. The numerical simulations were carried out using the PlymGrid facility at the University of Plymouth.

[1] K. G. Wilson, Phys. Rev. D **10**, 2445 (1974).
[2] D. J. Gross, I. R. Klebanov, A. V. Matytsin, and A. V. Smilga, Nucl. Phys. **B461**, 109 (1996).
[3] M. Albanese *et al.* (APE Collaboration), Phys. Lett. B **192**, 163 (1987).
[4] M. Teper, Phys. Lett. B **183**, 345 (1987).
[5] G. S. Bali and K. Schilling, Phys. Rev. D **46**, 2636 (1992).
[6] M. Lavelle and D. McMullan, Phys. Rep. **279**, 1 (1997).
[7] P. A. M. Dirac, Can. J. Phys. **33**, 650 (1955).
[8] R. Horan, M. Lavelle, and D. McMullan, Pramana **51**, 317 (1998).
[9] E. Bagan, M. Lavelle, and D. McMullan, Ann. Phys. (N.Y.) **282**, 471 (2000); **282**, 503 (2000).
[10] A. Ilderton, M. Lavelle, and D. McMullan, J. High Energy Phys. 03 (2007) 044.
[11] E. Marinari, M. L. Paciello, G. Parisi, and B. Taglienti, Phys. Lett. B **298**, 400 (1993).
[12] J. Greensite and S. Olejnik, Phys. Rev. D **67**, 094503 (2003).
[13] V. N. Gribov, Nucl. Phys. **B139**, 1 (1978).
[14] I. M. Singer, Commun. Math. Phys. **60**, 7 (1978).
[15] Note that in order to conform to lattice conventions, the gauge transformations have been renamed $h \rightarrow h^{\dagger}$ etc. as compared to [6,8–10].
[16] P. E. Haagensen and K. Johnson, arXiv:hep-th/9702204.
[17] The generalization to moving charges is discussed in detail in [9].
[18] M. Lavelle and D. McMullan, Phys. Lett. B **436**, 339 (1998).
[19] Working in an arbitrary covariant gauge in this way allows us to check the gauge invariance of the construction. It also allows us to avoid the need for Dirac bracket commutators that arise in, for example, Coulomb gauge.
[20] E. Bagan, M. Lavelle, D. McMullan, and S. Tanimura, Phys. Rev. D **65**, 105004 (2002).
[21] E. Bagan, M. Lavelle, and D. McMullan, Phys. Lett. B **477**, 355 (2000).
[22] E. Bagan, M. Lavelle, and D. McMullan, Phys. Lett. B **632**, 652 (2006).
[23] M. Lavelle and D. McMullan, Phys. Lett. B **471**, 65 (1999).
[24] L. Susskind, in *Weak and Electromagnetic Interactions At*

High Energy, Proceedings of the Les Houches Summer School 1976, edited by R. Balian and C. H. L. Smith (North-Holland, Amsterdam, 1977).
[25] J. B. Kogut, Rev. Mod. Phys. **55**, 775 (1983).
[26] W. Fischler, Nucl. Phys. **B129**, 157 (1977).
[27] M. Peter, Nucl. Phys. **B501**, 471 (1997).
[28] Y. Schroder, Phys. Lett. B **447**, 321 (1999).
[29] I. B. Khriplovich, Yad. Fiz. **10**, 409 (1969) [Sov. J. Nucl. Phys. **10**, 235 (1970)].
[30] A. Duncan, Phys. Rev. D **13**, 2866 (1976).
[31] J. Frenkel and J. C. Taylor, Nucl. Phys. **B109**, 439 (1976); **B155**, 544(E) (1979).
[32] T. Appelquist, M. Dine, and I. J. Muzinich, Phys. Lett. **69B**, 231 (1977).
[33] T. Appelquist, M. Dine, and I. J. Muzinich, Phys. Rev. D **17**, 2074 (1978).
[34] N. H. Christ and T. D. Lee, Phys. Rev. D **22**, 939 (1980).
[35] H. Nachbagauer, Phys. Rev. D **52**, 3672 (1995).
[36] H. Cheng and E. C. Tsai, Phys. Rev. Lett. **57**, 511 (1986); Phys. Rev. D **36**, 3196 (1987).
[37] P. J. Doust and J. C. Taylor, Phys. Lett. B **197**, 232 (1987).
[38] P. Doust, Ann. Phys. (N.Y.) **177**, 169 (1987).
[39] F. Halzen and A. D. Martin, *Quarks and Leptons: An Introductory Course in Modern Particle Physics* (Wiley & Sons, New York, 1984), Chap. 7.
[40] Y. L. Dokshitzer and D. E. Kharzeev, Annu. Rev. Nucl. Part. Sci. **54**, 487 (2004).
[41] A. Cucchieri and D. Zwanziger, Phys. Rev. D **65**, 014001 (2001).
[42] A. Cucchieri and D. Zwanziger, Phys. Lett. B **524**, 123 (2002).
[43] K. Langfeld and L. Moyaerts, Phys. Rev. D **70**, 074507 (2004).
[44] J. Greensite, S. Olejnik, and D. Zwanziger, Phys. Rev. D **69**, 074506 (2004).
[45] A. Nakamura and T. Saito, Prog. Theor. Phys. **115**, 189 (2006).
[46] Y. Nakagawa, A. Nakamura, T. Saito, H. Toki, and D. Zwanziger, Phys. Rev. D **73**, 094504 (2006).
[47] D. Zwanziger, Phys. Rev. Lett. **90**, 102001 (2003).
[48] A. P. Szczepaniak and E. S. Swanson, Phys. Rev. D **65**, 025012 (2001).
[49] A. P. Szczepaniak, Phys. Rev. D **69**, 074031 (2004).
[50] C. Feuchter and H. Reinhardt, Phys. Rev. D **70**, 105021 (2004).
[51] C. S. Fischer and D. Zwanziger, Phys. Rev. D **72**, 054005 (2005).
[52] J. Fingberg, U. M. Heller, and F. Karsch, Nucl. Phys. **B392**, 493 (1993).
[53] P. de Forcrand, J. E. Hetrick, A. Nakamura, and M. Plewnia, Nucl. Phys. B, Proc. Suppl.**20**, 194 (1991).
[54] J. Greensite, Prog. Part. Nucl. Phys. **51**, 1 (2003).